Proceedings of the ASME 2011 9th Fuel Cell Science, Engineering and Technology Conference
FuelCell2011
August 7-10, 2011, Washington, DC, USA

FuelCell2011-54838

Effect of Porosity Gradient in Gas Diffusion Layer on Cell Performance with Thin-Film Agglomerate Model in Cathode Catalyst Layer of a PEM Fuel Cell

Chun-I Lee, Shiqah-Ping Jung, Kan-Lin Hsueh, Chi-Chang Chen, Wen-Chen Chang

Green Energy and Environment Research Lab., Industrial Technology Research Institute, Hsinchu 310, Taiwan

ABSTRACT

A one-dimensional, steady-state, two-phase, isothermal numerical simulations were performed to investigate the effect on cell performance of a PEM fuel cell under non-uniform porosity of gas diffusion layer. In the simulation, the non-uniform porosity of gas diffusion layer was taken into account to analyze the transport phenomena of water flooding and mass transport in the gas diffusion layer. The porosity of the gas diffusion layer is treated as a linear function. Furthermore, the structure of the catalyst layer is considered to be a cylindrical thin-film agglomerate.

Regarding the distribution analysis of liquid water saturation, oxygen concentration and water concentration depend on the porosity of gas diffusion layer. In the simulation, the ε_{CG} and ε_{GC} represent the porosity of the interfaces between the channel and gas diffusion layer and the gas diffusion layer and the catalyst layer, respectively. The simulation results indicate that when the (ε_{CG}, ε_{GC}) = (0.8, 0.4), higher liquid water saturation appears in the gas diffusion layer and the catalyst layer. On the contrary, when the (ε_{CG}, ε_{GC}) = (0.4, 0.4), lower liquid water saturation appears. Once the liquid water produced by the electrochemical reaction and condensate of vapor water may accumulate in the open pores of the gas diffusion layer and reduced the oxygen transport to the catalyst sites. This research attempts to use a thin-film agglomerate model, which analyze the significant transport phenomena of water flooding and mass transport under linear porosity gradient of gas diffusion layer in the cathode of a PEM fuel cell.

Keywords: PEM fuel cell, thin-film agglomerate model, gas diffusion layer, porosity gradient

INTRODUCTION

The proton exchange membrane (PEM) fuel cell is a type of lower temperature fuel cells and has been regarded as promising candidate of future power sources for stationary, portable, and automotive applications [1]. The fuel cell has many important features such as high-energy efficiency, low noise, low emission, and low operating temperature (i.e., quick start-up at ambient temperature). Several literature reports intend to enhance the performance of PEM fuel cell. The cell performance is critically depending on the catalyst activity in the catalyst layer and the optimal design configuration of the catalyst layer.

The gas diffusion layer (GDL), as a component of the membrane electrode assembly, plays an important role in the PEM fuel cell through affecting the diffusion of reactants and water as well as the conduction of electrons [2-6]. Water accumulated in the GDL reduces the porosity of GDL, causes the flooding of electrode, and retards the transport of reactants to the catalyst layer. Gurau et al. [7] developed an analytical solution for a half-cell model. The discrete porosity is adopted for the GDL. Results showed how the limiting current density and electrode polarization were effects by the fraction of liquid volume. Chu et al. [8] investigated the effect of the non-uniform porosity of GDL on the performance with various testing parameters. Several complicated models have been developed to demonstrate the influence of the two-phase flow in the diffusion media. Nguyen and his co-worker were one of the pioneers investigating two-phase flow. They clearly indicated that water saturation has a significant effect on the cathode performance. Their two-phase models used empirical expression for the saturation function [9-13]. Wang [14-17] conducted a numerical study to investigate the effects of GDL flooding with various flow configuration, GDL structural, reaction rate, and fuel cell operating in cold start.

Zhan et al. [18] used a two-phase flow model for the fuel cell electrode to show that a GDL with a porosity gradient improves the liquid water removal from the

catalyst layer. Tang et al. [19] experimentally investigated the effect of a porosity-graded micro porous layer on cell performance. Results revealed that the improved performance is probably due to fast water transport through large pores and gas diffusion through the small pores. Kong et al. [20] also found that the pore-size distribution is an important structural parameter affecting the cell performance as well as the total porosity.

Several researchers proposed that the agglomerate model might be the best among other models for simulation of catalyst layer of a real PEM fuel cell. Iczkowski and Cutlip [21] considered cylindrical agglomerates and this model considered the diffusion of oxygen, nitrogen, and water in the gas-filled pores of a PEM fuel cell. The reactant gas diffuses through this porous film to the catalyst, where the electrochemical reactions occur. Chang and Chu [22, 23] presented a one-dimensional, two-phase transient model. They investigated the critical parameters and the operating conditions for cylindrical and spherical agglomerates in the cathode catalyst layer of a PEM fuel cell. Lin *et al*. [24] presented a one-dimensional, two-phase, steady state, isothermal model for a PEM fuel cell cathode. Their simulation results revealed that the operating parameters affected the water generation and removal process.

These studies mentioned have recognized that a porosity gradient in the GDL on the cathode side will enhance the transport of the gas reactants and increase the remove of the water in a PEM fuel cell. Therefore, the purpose of the present study is to investigate the transport phenomena of water flooding and mass transport under non-uniform porosity of GDL in the cathode of a PEM fuel cell.

DESCRIPTION OF THE MODEL

The physical model employed in this study consists of three parts, namely a GDL, a catalyst layer, and a polymer membrane on the cathode side of the PEM fuel cell, as illustrated in Fig.1. In the catalyst layer, cylindrical pellet geometry is used to describe the catalyst composite, which combines features of the thin-film and agglomerate models. Porosity of the GDL is assumed non-uniform. The gas inlet position (x = 0) is defined at the interface between the flow channel and the GDL. The position at x = L is located at the interface between the membrane and anode.

Assumptions

This model incorporates following assumptions:

1. The system operates in a steady state, isothermal, and isobaric process.
2. All the gases behave as ideal gas and the liquid water is incompressible.
3. The electronic resistance of the GDL and catalyst layer is negligible.
4. The membrane is impermeable to gaseous species.
5. The catalyst pellets are homogeneous.
6. The catalyst pellet radius, Nafion film thickness, and water film thickness are constant.
7. The water produced by the oxygen reduction reaction on the cathode is in liquid form.

Conservation Equations

The main governing equations are listed on Table I. The flux (N_i) for the gas "i" is

$$N_i = -D_i\left[\varepsilon_i(1-s)\right]^{1.5}\nabla C_i \tag{1}$$

Where the subscript "*i*" is denote for oxygen or vapor. The ε_i is the porosity of the GDL or the catalyst layer. In this study, the porosity in the GDL is a linear function of ε_{CG} and ε_{GC}.

$$\varepsilon_{GDL}(j) = \varepsilon_{GC} + t_{GDL}((\varepsilon_{CG} - \varepsilon_{GC})/H_{GDL}) \tag{2}$$

The ε_{CG} is the porosity at the interfaces between flow channel and GDL. The ε_{GC} is the porosity at the interface between the GDL and the catalyst layer. The H_{GDL} is the thickness of GDL. Note that in this study, to enhance the performance of the PEM fuel cell, we let $\varepsilon_{CG} \geqq \varepsilon_{GC}$.

The interfacial transfer rate between vapor and water, R_w, is a simplified switch function between condensation and/or evaporation of water as given by equation (3).

$$R_w = \begin{cases} k_c \dfrac{\varepsilon_i(1-s)x_w}{RT}(x_w P - P_{sat}), & if \quad x_w P > P_{sat} \\ k_v \dfrac{\varepsilon_i s \rho_w}{M_w}(x_w P - P_{sat}), & if \quad x_w P < P_{sat} \end{cases} \tag{3}$$

Where k_c and k_v are the condensation and evaporation rate constants, respectively. The x_w is the molar fraction of water vapor, the M_w is molecular weight of water, and the P_{sat} is the saturation pressure of water. It is temperature dependant.

In the catalyst layer, R_{O2} represents the oxygen reduction rate within the catalyst pellet. It is derived from Thiele modulus method and is given by

$$R_{O_2} = \frac{RT/H^N_{O_2}}{\dfrac{\delta_N}{a_r D^N_{O_2}} + \dfrac{\delta_w}{a_r D^w_{O_2}}\dfrac{H^w_{O_2}}{H^N_{O_2}} + \dfrac{1}{\xi k_T}} C^g_{O_2} \tag{4}$$

Where $H^w_{O_2}$ represents Henry's constant of oxygen between air and liquid water. The $H^N_{O_2}$ is Henry's constant of oxygen between air and the Nafion phase. The $D^w_{O_2}$ and $D^N_{O_2}$ represent oxygen diffusivity in liquid water and the oxygen diffusivity in Nafion phase, respectively. The a_r is the outer surface area of the agglomerates per unit volume of the catalyst layer as given by equation (5).

$$a_r = \frac{2}{r_P + \delta_N}(1-\varepsilon_0^{CL}) \tag{5}$$

Where r_P and δ_N are denote for the radius of the catalyst

pellets and for the Nafion film thickness, respectively.

The reaction rate constant k_T is expressed by the Tafel equation:

$$k_T = \left(1-\varepsilon_0^{CL}\right)\frac{1}{4FC_{O_2,ref}}a_{Pt}^{agg}i_0\exp\left[-\frac{2.303\left(V_s-\phi-U_{ref}\right)}{b}\right] \quad (6)$$

where a_{Pt}^{agg} is the active catalyst surface area per unit volume of agglomerates and is expressed as:

$$a_{Pt}^{agg} = \frac{a_{Pt}m_{Pt}}{\delta_{CL}\left(1-\varepsilon_0^{CL}\right)} \quad (7)$$

For the cylindrical, the effectiveness factor (ξ) is denoted by

$$\xi = \frac{1}{\varphi}\frac{3\varphi\coth(3\varphi)-1}{3\varphi} \quad (8)$$

Where φ represents the Thiele modulus and is given by

$$\varphi = \frac{r_P}{2}\sqrt{\frac{k_T/\left(1-\varepsilon_0^{CL}\right)}{D_{O_2,eff}^N}} \quad (9)$$

Capillary force dominates the transport of liquid water in the porous media. Therefore, present model uses Darcy's Law to describe the flow of liquid water in these porous media. The liquid water flux is expressed by:

$$N_w = -\frac{\rho_w K_w(s)}{M_w\mu_w}\nabla P_l \quad (10)$$

The transport of liquid water is dominated by water concentration gradient and electro-osmotic drag, which is given by:

$$N_w = \frac{i_+}{F}n_d - D_w^N\nabla C_w^N \quad (11)$$

Initial and Boundary Conditions

Initial conditions and boundary conditions are necessary and crucial for solving governing equations mentioned above. They are described in the following.

- *At the gas channel boundary (x=0)*

The inlet molar concentration is determined by the inlet pressure, the temperature, and the humidity, according to the ideal gas law. Therefore, the concentrations of oxygen and vapor water are

$$C_{O_2}^g = C_{O_2}^{air} \quad (12a)$$

$$C_v^g = C_v^{air} \quad (12b)$$

The liquid water saturation level is

$$s = s_0 \quad (13)$$

- *At the interface between GDL and catalyst layer*

The concentrations of oxygen and vapor water at this interface are

$$N_{O_2}^g\Big|_{GDL} = N_{O_2}^g\Big|_{CL} \quad (14a)$$

$$N_v^g\Big|_{GDL} = N_v^g\Big|_{CL} \quad (14b)$$

The liquid water saturation level and liquid water flux at this interface are

$$N_w\big|_{GDL} = N_w\big|_{CL} \quad (15a)$$

$$C_w^N = 0 \quad (15b)$$

The ionic potential is set to be zero.

$$i_+\big|_{CL} = 0 \quad (16)$$

- At the interface between catalyst layer and membrane

The concentrations of oxygen and vapor water are

$$N_v^g\Big|_{CL} = 0 \quad (17a)$$

$$N_{O_2}^g\Big|_{CL} = 0 \quad (17b)$$

The liquid water saturation level and liquid water flux are

$$N_w\big|_{CL} = N_w\big|_{MEM} \quad (18a)$$

$$C_w^N = C_{w(\alpha)}^{N,eq} \quad (18b)$$

The ionic potential and ionic current is continuous at this interface.

$$i_+\big|_{CL} = i_+\big|_{MEM} \quad (19)$$

- At the interface between membrane and catalyst layer on the anode side

The concentrations of oxygen and vapor are

$$C_{O_2}^g = 0 \quad (20a)$$

$$C_v^g = 0 \quad (20b)$$

The liquid water saturation level and water flux are

$$s = 0 \quad (21a)$$

$$C_w^N = C_{w(\alpha^{anode})}^{N,eq} \quad (21b)$$

The ionic potential is approximately zero due to rapid hydrogen oxidation rate.

$$\phi = 0 \quad (22)$$

RESULTS AND DISCUSSION

Present study established a one-dimension PEM fuel cell model to simulate the water flooding phenomena and mass transport process inside a GDL with non-uniform porosity. The effects of porosity gradient on cell performance are also elucidated. Table II listed the major geometric dimensions and physical properties. Six cases with different porosity gradients were studied. Those porosity gradients were (ε_{CG}, ε_{GC}) = (0.8, 0.8), (0.8, 0.6), (0.8, 0.4), (0.6, 0.6), (0.6, 0.4), and (0.4, 0.4).

The inlet molar concentrations of individual species were calculated from the inlet pressure, the temperature, and the humidity, according to the ideal gas law. The membrane/anode interface condition was assumed to be fully humidified and the cell temperature is a constant at 333 K.

Figure 2 plots the polarization curve at various porosity gradients of GDL of cathode. Among six cases, the case with porosity of ε_{CG}=0.8 and ε_{GC}=0.8 leads to the

highest current density. Whereas the case with the porosity of ε_{CG}=0.4 and ε_{GC}=0.4 yields the lowest current density at 0.2 V. Current density at this voltage was mainly affected by the concentration over-potential or in the other words, the mass transport process in the electrode. Water is more difficult to transport in the GDL with low porosity than the GDL with high porosity. Water tends to accumulate in the electrode with low porosity GDL. For porosity gradient GDL, the cell performance with porosity gradient of ε_{CG}=0.8 and ε_{GC}=0.6 was higher than the porosity gradient of ε_{CG}=0.8 and ε_{GC}=0.4 or ε_{CG}=0.6 and ε_{GC}=0.4. Tang et al. [25] indicated that GDL with low porosity region near the catalyst layer and high porosity region near flow channel results a net pulling force of water from catalyst layer through GDL to the flow channel. However, if the porosity gradient is opposite, the water cannot expel from the GDL. Accumulated water blocks the pathway of fuel, causes the reduction of fuel supply, and reduced output current density.

Figure 3 and 4 show the distributions of oxygen concentration and vapor inside cathode for six cases at a cell voltage of 0.2 V. The vertical dotted line indicates the interface between the GDL and catalyst layer. The results reveal that the oxygen concentration gradually decreases along the x-direction owing to the consumption of oxygen in the cathode catalyst layer. Therefore, low oxygen concentration appears in the catalyst layer of each case. On the contrary, the concentration of water vapor gradually increases owing to the production of water in the cathode catalyst layer. The oxygen concentrations in the case of ε_{CG}=0.8 and ε_{GC}=0.8 is the highest among other cases. This is due to low water accumulation inside GDL. The phenomena of oxygen concentration distribution in the CL show the similar trend to the study of Wang [17].

Fig. 5 is the profiles of water saturation level of six cases at cell voltage of 0.2 V. Results reveal that the water saturation is discontinuous at the interface between GDL and catalyst layer. The capillary pressure is continuous at the interface. However, the discontinuous of porosity, permeability, and contact angle at the interface causes discontinue of water saturation profile. Moreover, from Fig. 5, it can clearly be seen that the liquid water saturation level of the GDL with porosity of ε_{CG}=0.8 and ε_{GC}=0.4 is the highest among other cases. On the contrary, the water saturation level of the GDL with porosity of ε_{CG}=0.8 and ε_{GC}=0.8 is lowest. This result represents that the GDL with high porosity offers pathway for oxygen transport, decreases the oxygen diffusion resistance in the GDL, and improves the cell performance.

CONCLUSIONS

A one-dimensional, steady-state, two-phase, isothermal PEM fuel cell model has been developed to investigate the transport phenomena of water inside cathode, flooding level, oxygen diffusion, and cell performance. GDL in the mode has non-uniform porosity. The simulation results show that the GDL porosity of ε_{CG}=0.8 and ε_{GC}=0.8 has a better performance than others. The GDL with porosity of ε_{CG}=0.8 and ε_{GC}=0.4 has a lower cell performance than others. This is due to that GDL with low porosity region near the catalyst layer and high porosity region near flow channel results a net pulling force of water from catalyst layer through GDL to the flow channel. Accumulation of water inside GDL reduces cell performance. Water blocks the pathway of fuel, causes the reduction of fuel supply, and reduced output current density.

ACKNOWLEDGES

The authors would like to thank the Bureau of Energy, Ministry of Economic Affairs of Republic of China for financial support. This research was carried out under contract number 100-D0212.

REFERENCES

[1] J. Thepkaew, A. Therdthianwong, S. Therdthianwong, Key parameters of active layers affecting proton exchange membrane (PEM) fuel cell performance, Energy 33 (2008) 1794-1800.

[2] A. Therdthianwong, P. Manomayidthikarn, S. Therdthianwong, Investigation of membrane electrode assembly (MEA) hot-pressing parameters for proton exchange membrane fuel cell, Energy 32 (2007) 2401-2411.

[3] U. Pasaogullari, C. Wang, Two-phase transport and the role of micro-porous layer in polymer electrolyte fuel cells, Electrochimica Acta 49 (2004) 4359-4369.

[4] W. Sun, B. Peppley, K. Karan, Influence of gas diffusion layer and channel geometry parameters on catalyst performance: Investigation using a 2-D model, J. Power Sources 144 (2005) 42-53.

[5] C. Lim, C. Wang, Effects of hydrophobic polymer content in GDL on power, Electrochimica Acta 49 (2004) 4149-4156.

[6] J.Y. Jang, C.H. Cheng, Y.H. Huang, Optimal design of baffles locations with interdigitated flow channels of a centimeter-scale proton exchange membrane fuel cell, *Int. J. Heat and Mass Trans.* 53 (2010) 732-743.

[7] V. Gurau, F. Barbir, H.T. Liu, An analytical solution of a half-cell model for PEM fuel cells. *J. Electrochem. Soc.* 147(7) (2000) 2468-2477.

[8] H.S. Chu, C. Yeh, F. Chen, Effects of porosity change of gas diffuser on performance of proton exchange membrane fuel cell. *J. Power Sources* 123(1) (2003) 1-9.

[9] J.S. Yi, T.V. Nguyen, Multicomponent transport in porous electrodes of proton exchange membrane fuel cells using the interdigitated gas distributors. *J. Electrochem. Soc.* 146(1) (1999) 38-45.

[10] W.S. He, J.S. Yi, T.V. Nguyen, Two-phase flow model of the cathode of PEM fuel cells using interdigitated flow fields. *AIChE Journal* 46(10)

(2000) 2053-2064.
[11] D.L. Wood, Y.S. Yi, T.V. Nguyen, Effect of direct liquid water injection and interdigitated flow field on the performance of proton exchange membrane fuel cells. *Electrochimica Acta* 43(24) 1998 3795-3809.
[12] D. Natarajan, T.V. Nguyen, A two-dimensional, two-phase, multicomponent, transient model for the cathode of a proton exchange membrane fuel cell using conventional gas distributors. *J. Electrochem. Soc.* 148(12) (2001) A1324-A1335.
[13] D. Natarajan, T.V. Nguyen, Three-dimensional effects of liquid water flooding in the cathode of a PEM fuel cell. *J. Power Sources* 115(1) (2003) 66-80.
[14] Y. Wang, Modeling of two-phase transport in the diffusion media of polymer electrolyte fuel cells. *J. Power Sources* 185 (2008) 261-271.
[15] Y. Wang, C.Y. Wang, K.S. Chen, Elucidating Differences between Carbon Paper and Carbon Cloth in Polymer Electrolyte Fuel Cells. *Electrochimica Acta* 52 (2007) 3965-3975.
[16] Y. Wang, X. Feng, Analysis of Reaction Rates in the Cathode Electrode of Polymer Electrolyte Fuel Cells Part I: Single-Layer Electrodes. *J. Electrochem. Soc.* 155(12) (2008) B1289-B1295.
[17] Y. Wang, Analysis of the Key Parameters in the Cold Start of Polymer Electrolyte Fuel Cells. *J. Electrochem. Soc.* 154 (2007) B1041-B1048.
[18] Z.G. Zhan, J.S. Xiao, D.Y. Li, M. Pan, R. Yuan, Effects of porosity distribution variation on the liquid water flux through gas diffusion layers of PEM fuel cells. *J. Power Sources* 160 (2006) 1041-1048.
[19] H. Tang, S. Wang, M. Pan, R. Yuan, Porosity-graded micro-porous layers for polymer electrolyte membrane fuel cells. *J. Power Sources* 166 (2007) 41-46.
[20] C.S. Kong, D.Y. Kim, H.K. Lee, Y.G. Shul, T.H. Lee, Influence of pore-size distribution of diffusion layer on mass-transport problems of proton exchange membrane fuel cells. *J. Power Sources* 108 (2002) 185-191.
[21] R.P. Iczkowski, M.B. Cutlip, Voltage Losses in Fuel Cell Cathodes. *J. Electrochem. Soc.* 127 (1980) 1433-1440.
[22] S.M. Chang, H.S. Chu, Transient behavior of a PEMFC. *J. Power Sources* 161 (2006) 1161-1168.
[23] S.M. Chang, H.S. Chu, A transient model of PEM fuel cells based on a spherical thin film-agglomerate approach. *J. Power Sources* 172 (2007) 790-798.
[24] G. Lin, W. He, T.V. Nguyen, Modeling Liquid Water Effects in the Gas Diffusion and Catalyst Layers of the Cathode of a PEM Fuel Cell. *J. Electrochem. Soc.* 151 (2004) A1999-A2006.
[25] H. Tang, S. Wang, M. Pan, R. Yuan, Porosity-graded micro-porous layers for polymer electrolyte membrane fuel cells. *J. Power Sources* 166 (2007) 41-46.

Table I. Governing equations

Variables	GDL	CL	MEN
$C_{O_2}^g$	$D_{O_2}\varepsilon_0^{GDL^\tau}\left[(1-s)^\tau\nabla^2 C_{O_2}^g+\nabla\cdot(1-s)^\tau\nabla\cdot C_{O_2}^g\right]=0$	$D_{O_2}\varepsilon_0^{CL^\tau}\left[(1-s)^\tau\nabla^2 C_{O_2}^g+\nabla\cdot(1-s)^\tau\nabla\cdot C_{O_2}^g\right]-R_{O_2}=0$	$C_{O_2}^g=0$
C_v^g	$D_v\varepsilon_0^{GDL^\tau}\left[(1-s)^\tau\nabla^2 C_v^g+\nabla\cdot(1-s)^\tau\nabla C_v^g\right]-R_w=0$	$D_v\varepsilon_0^{CL^\tau}\left[(1-s)^\tau\nabla^2 C_v^g+\nabla\cdot(1-s)^\tau\nabla\cdot C_v^g\right]-R_w=0$	$C_v^g=0$
ϕ	N/A	$\kappa_{N,eff}\nabla^2\phi-4FR_{O_2}=0$	$\nabla^2\phi=0$
s	$\frac{\rho_w K_{w,0}}{M_w\mu_w}\left(-\frac{dP_c}{ds}\right)\left[s\nabla^2 s+(\nabla\cdot s)^2\right]+R_w=0$	$\frac{\rho_w K_{w,0}}{M_w\mu_w}\left(-\frac{dP_c}{ds}\right)\left[s\nabla^2 s+(\nabla\cdot s)^2\right]+\left(4n_d^{CL}+2\right)R_{O_2}+R_w=0$	$s=0$
C_w^N	N/A	$\nabla^2 C_w^N=0$	$D_w^N\nabla^2 C_w^N+\frac{n_d\kappa_n}{F}\nabla^2\phi=0$

Table II. Summary of parameters in the simulation

GDL properties	
Thickness (δ_{GDL})	0.025 cm
Liquid water permeability at 100% saturation (K_0^{GDL})	10^{-9} cm^2
CL properties	
Porosity (ε_0^{CL})	0.06
Thickness (δ_{CL})	0.0016 cm
Liquid water permeability at 100% saturation (K_0^{CL})	3×10^{-11} cm^2
Catalyst loading (m_{Pt})	0.4 mg cm^{-2}
Specific surface area of Pt (a_{Pt})	1000 cm^2 mg^{-1}
Volumetric fraction of Nafion in catalyst pellet (ε_N^p)	0.393
Volumetric fraction of carbon in catalyst pellet (ε_C^p)	0.469
Radius of catalyst pellet (r_P)	10^{-5} cm
Thickness of Nafion film (δ_N)	10^{-6} cm
MEM properties	
Thickness (δ_{MEM})	0.005 cm

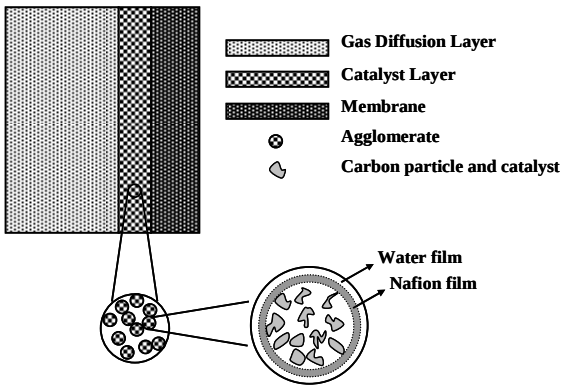

Figure 1 Schematic structure of PEM fuel cell and computational domain.

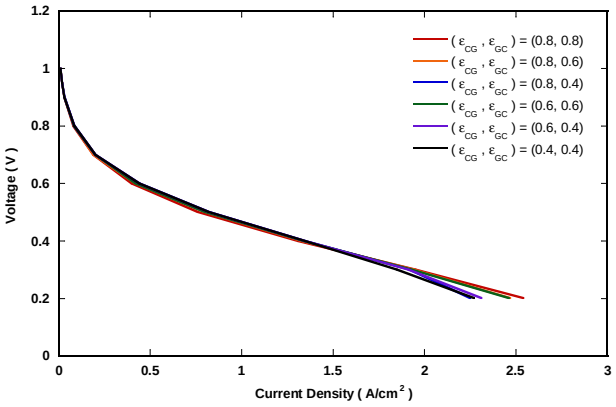

Figure 2 The polarization curve at various porosity gradients of GDL of cathode.

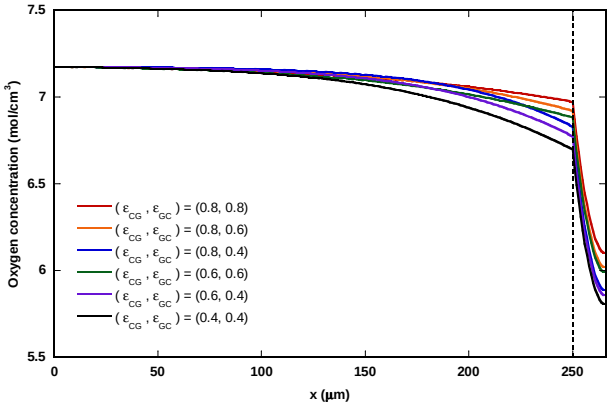

Figure 3 Distributions of oxygen concentration inside cathode with different porosities at a cell voltage of 0.2 V.

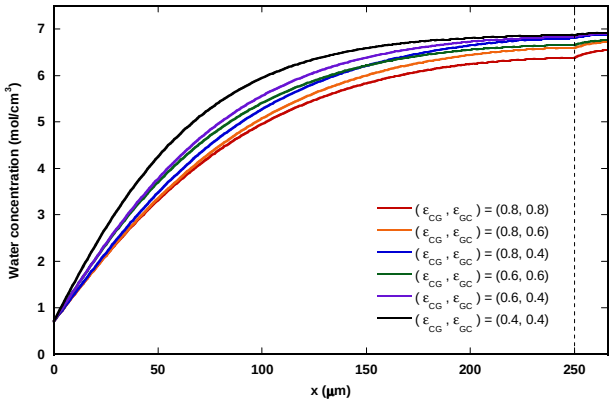

Figure 4 Distributions of vapor inside cathode with different porosities at a cell voltage of 0.2 V.

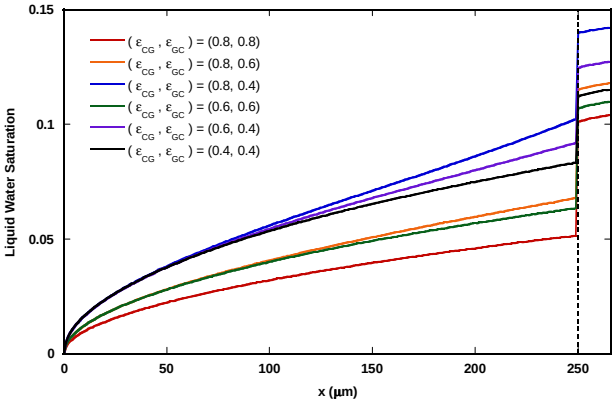

Figure 5 Liquid water saturation profiles inside cathode with different porosities for six cases at a cell voltage of 0.2 V.